

# Motion Control of a Three Active Wheeled Mobile Robot and Collision-Free Human Following Navigation in Outdoor Environment

Yousif E. Abdelgabar, Jae Hoon Lee, *Member, IAENG*, and Shingo Okamoto

**Abstract**— In this paper, design of a steering mechanism for a three wheeled mobile robot, kinematic modeling, system motion control, and collision-free algorithm for human following were presented. During high speed target following navigation, sometimes vibration problem occurred in the robot's passive front wheel. To reduce the vibration and to get a better performance in high speed navigation, an active steering wheel was developed. The proposed motion control method of the new platform was explained and validated through experiments. Also a collision-free human following algorithm considering static and dynamic obstacles was introduced and demonstrated experimentally in this research.

**Index Terms**— Human following, Redundant actuation, Collision avoidance, Laser scanner

## I. INTRODUCTION

RECENTLY, interest is growing in the potential of human symbiotic robots such as daily life support robots that can care for the aged, young children and needy people in our everyday environments.

For the purposes of this research, only outdoor circumstances are considered. Outdoor environments are considered challenging because they are rapidly changing. Therefore, an outdoor robot needs to be able to safely fulfill its functions in such environments. To ensure safely navigation, the robot should be guided to the desired destinations and prevent any undesired behaviors at the same time. To achieve this we need to develop stable robot platforms and also a reliable control method. Many researches dealt with developing of stable mobile robot platforms and discussed many kinematic models [1]-[3].

Coexistence of robots and humans has been one of the vital fields of research. For a successful coexistence the robot is required to have the capability to collaborate with humans. For that, the robot should be able to recognize humans and move safely in various environments. A mobile robot that can follow a running person and avoid collision with static and dynamic obstacles can be considered as a real representative application of these technologies.

Recently, there have been many studies on coexistence of robots and humans. For example, Fox introduced a method called dynamic window approach for collision avoidance [4].

Manuscript received December 11, 2015; revised December 22, 2015.

All authors are with Mechanical Engineering Course, Graduate School of Science and Engineering, Ehime University, 3 Bunkyo-cho, Matsuyama 790-8577, Japan.

Yousif E. Abdelgabar (e-mail: b840039u@mails.cc.ehime-u.ac.jp).

Jae Hoon Lee (e-mail: lee.jaehoon.mc@ehime-u.ac.jp).

Shingo Okamoto (e-mail: okamoto.shingo.mh@ehime-u.ac.jp).

Collision avoidance methods based on the potential field approach were also investigated [5], [6]. Also, fuzzy logic based collision free navigation algorithms were investigated [7], [8]. Some researchers investigated and tested many approaches to track and follow a moving target [9]-[11].

The objective of this research is to modify the robot platform with an active steering front wheel, develop the motion control method for the modified system, and introduce a simple collision-free human following navigation algorithm in outdoor environment that can follow a moving target person and avoid collision with static and dynamic obstacles.

## II. MODIFICATION OF THE MOBILE ROBOT SYSTEM

### A. Mobile Robot System

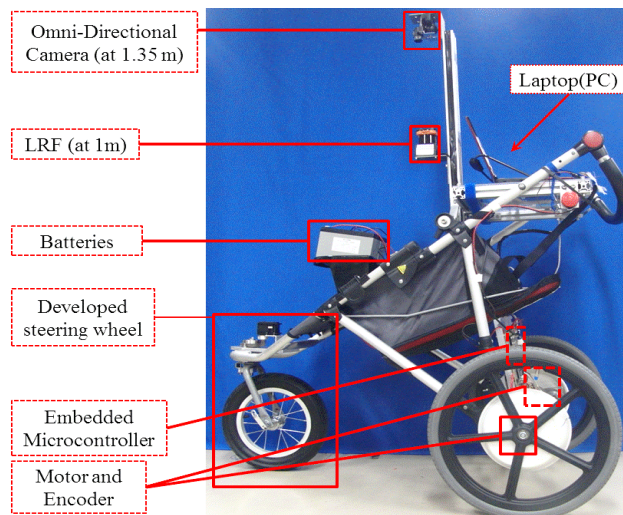


Fig. 1. Mobile robot system

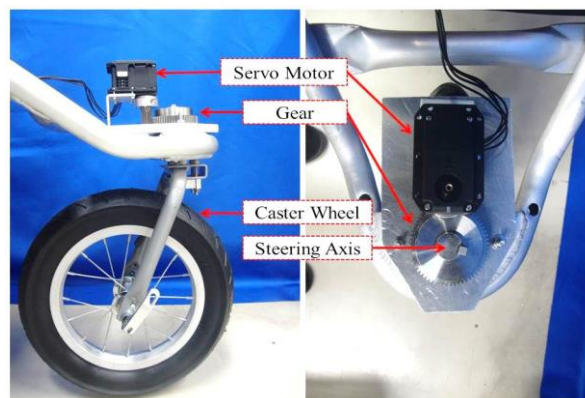


Fig. 2. Developed steering wheel of the robot

The modified mobile robot is shown in Fig. 1. The mobile robot equipped with a laser scanner and an omnidirectional camera which are used to recognize the target person and people around the robot. The information of both sensors and the odometer data of the robot are fused in real time by the filtering algorithm installed in the control system [11]. The developed steering wheel type, as shown in Fig. 2, is a backward offset steered wheel. The wheel is actuated by using a servo motor (dynamixel MX64, Robotis co.). The servo motor is connected to the main laptop computer using a USB cable through a configurator (BTE068). All three motors and the robot sensors are supplied with two 12[V] LEAD-ACID batteries. An embedded microcontroller (SH2) is used to control the two rear wheels of the robot. The encoders are used to measure the angle of rear wheels. Also the servo motor angle is used to measure the steering angle of the front wheel.

### B. Configuration of the Mobile Robot System

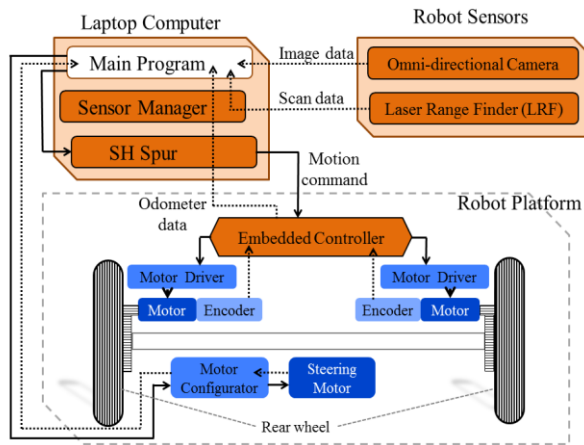


Fig. 3. Block diagram of the mobile robot system

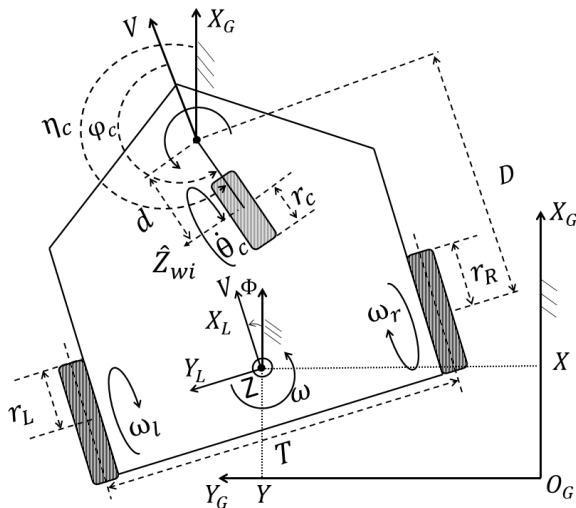


Fig. 4. Kinematic model of the three wheeled robot

Fig. 3 shows the system block diagram of the mobile robot. The block diagram has three main parts: sensors, laptop computer and mobile robot platform. All the sensors data are processed and used by the main program, which sends the commands to the microcontroller through the SH spur program. The microcontroller measures the both wheels angle and controls them. The encoders data of the rear wheels

is used by the SH spur program to calculate the robot's position and orientation and to control the platform. The servo motor has a built-in microcontroller that is used to control the motor and send the motor angle position to the main program. Then the main program calculates the steering axis velocity  $\dot{\phi}_c$  and sends the commands to the servo motor to give a steering angular velocity correspondent with the robot motion.

### C. Kinematic Model

We assume that there's no sliding and skidding friction between the wheels and the ground. Fig. 4 shows the kinematic model of the mobile robot. When we only consider the two rear wheels, the platform represents a differential drive robot. The linear velocity  $V$  and the angular velocity  $\omega$  of the robot can be calculated by using the following model.

$$\begin{bmatrix} V \\ \omega \end{bmatrix} = \begin{bmatrix} r_R & r_L \\ 2 & 2 \\ r_R & -r_L \\ T & -T \end{bmatrix} \begin{bmatrix} \omega_R \\ \omega_L \end{bmatrix} \quad (1)$$

Where,  $r_R$  and  $r_L$  denote the radius of the right and the left wheel respectively.  $T$  represents the distance between the both wheels.  $\omega_R$  and  $\omega_L$  denote the right and the left wheel rotational velocity, respectively.

Basically, the robot motion is controlled by the two rear wheels, and we need to control the front wheel angle to be correspondent with the robot motion. To do this, we need to drive the kinematic equation of the steering axis velocity  $\dot{\phi}_c$ . Now, let's consider the platform with only the caster wheel attached to it. The following equation describes the velocity relationship between the platform and the caster wheel [2].

$$\begin{pmatrix} V \\ 0 \\ \omega \end{pmatrix} = \begin{bmatrix} dS_{\phi_c} & r_c C_{\phi_c} & 0 \\ -dC_{\phi_c} - D & r_c S_{\phi_c} & D \\ 1 & 0 & -1 \end{bmatrix} \begin{pmatrix} \dot{\eta}_c \\ \dot{\theta}_c \\ \dot{\phi}_c \end{pmatrix} \quad (2)$$

Where,  $d$  represents the distance between the center of the caster wheel and the steering axis,  $r_c$  represents the radius of the caster wheel,  $\eta_c$  represents the steering angle with respect to the global coordinate system,  $\theta_c$  represents the rotational velocity of the front wheel,  $\phi_c$  represent the steering angle with respect to the robot coordinate system, and  $D$  represents the distance between the steering axis and the center point between the both rear wheels. Here,  $S_{\phi_c} = \sin\phi_c$  and  $C_{\phi_c} = \cos\phi_c$ . Also by using the above relationship we can obtain the inverse kinematic as follow.

$$\begin{pmatrix} \dot{\eta}_c \\ \dot{\theta}_c \\ \dot{\phi}_c \end{pmatrix} = \frac{1}{dr_c} \begin{bmatrix} r_c S_{\phi_c} & -r_c C_{\phi_c} & -Dr_c C_{\phi_c} \\ dC_{\phi_c} & dS_{\phi_c} & -DdS_{\phi_c} \\ r_c S_{\phi_c} & -r_c C_{\phi_c} & -dr_c - Dr_c C_{\phi_c} \end{bmatrix} \begin{pmatrix} V \\ 0 \\ \omega \end{pmatrix} \quad (3)$$

From the above equations the equation for the steering velocity is given as follow.

$$\dot{\phi}_c = \frac{1}{dr_c} \{r_c S_{\phi_c} V + (-dr_c - Dr_c C_{\phi_c}) \omega\}. \quad (4)$$

For the current system, velocity in  $Y$  direction  $\dot{Y}$  is equal to zero; velocity in  $X$  direction  $\dot{X}$  is the robot linear velocity  $V$ , and  $\dot{\phi}$  represents the robot angular velocity  $\omega$ .

### III. MOTION CONTROL

This section describes the method used to control the robot platform and the collision-free human following navigation algorithm.

#### A. Vehicle Motion Control

Fig. 5 shows the general flow chart for the vehicle motion control. After initialization, the robot either receives a motion command from external device, such as joystick, or determines the motion command needed for a certain desired motion (i.e, trajectory following). Then read the steering pose and calculate the steering axis velocity correspondent with the given linear and angular velocities. After that, send the calculated steering velocity to the joint axis servo motor and send the velocity command,  $V$  and  $\omega$ , to the SH spur program for platform motion control.

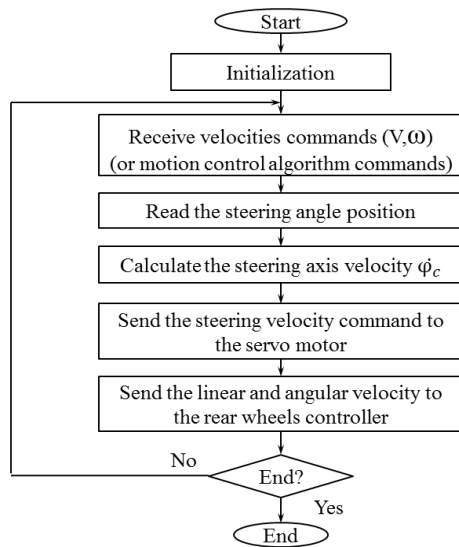


Fig. 5. Flow chart of the vehicle motion control

#### B. Human Following Algorithm

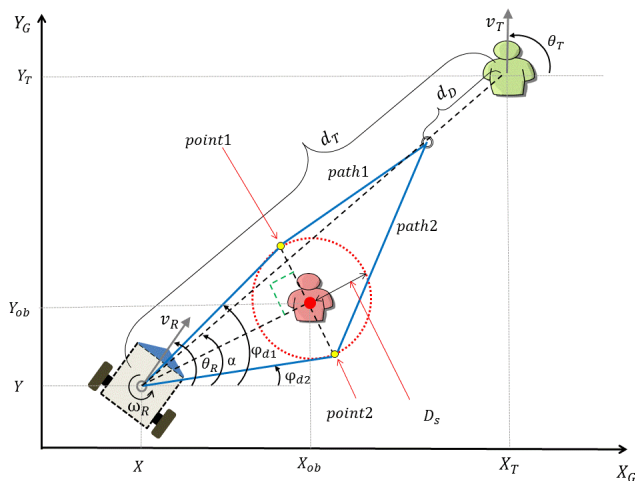


Fig. 6. Schematic representation of motion control to follow a target person considering an obstacle

Objects in close proximity to the robot are detected and tracked by sensors installed on the robot. The states of the target person and the obstacles are estimated using Kalman filtering method [11]. Fig. 6 shows the schematic representation of motion control to follow a target person considering an obstacle. For collision-free following

navigation, the robot is controlled based on the position relationship between the robot and the target as well as the obstacle. The desired linear velocity of the robot is computed based on the target velocity and the relative distance between the robot and the target person as follow.

$$v_R = v_T + K_v(d_T - d_D). \quad (5)$$

Where,  $v_T$  represents the velocity of the target person,  $d_T$  represents the distance between the robot and the target person,  $d_D$  represents the desired distance, and  $K_v$  represents the distance control feedback gain.

In outdoor environment they could be many obstacles around the robot and the goal point, from the robot point of view, is the distance ( $d_D$ ) behind the target. Therefore, the robot will not consider any obstacle farther than the target person.

If there is no obstacle between the robot and the target person, the robot angular velocity is decided based on the direction from the robot to the target person as follow.

$$\omega_D = K_1(\theta_T - \alpha) - K_2(\theta_R - \alpha). \quad (6)$$

Where,  $\theta_R$  and  $\theta_T$  denote the moving direction of the robot and the target person respectively.  $K_1$  and  $K_2$  denote the moving direction feedback gains. And  $\alpha$  denotes the direction from the robot to the target person with respect to the global coordinate system.

If any obstacle locates between the robot and the target person, the priority is to avoid the obstacle first. Otherwise, the robot continuous to follow the target person.

For obstacle avoidance, the desired heading  $\phi_d$  is determined geometrically by drawing a virtual circle around the obstacle using a virtual safety radius  $D_s$ . Therefore, the robot angular velocity is decided based on the  $\phi_d$  of the shortest path among the two possible paths around the obstacle as follow.

$$\omega_D = K_1(\theta_T - \phi_{di}) - K_2(\theta_R - \phi_{di}). \quad (7)$$

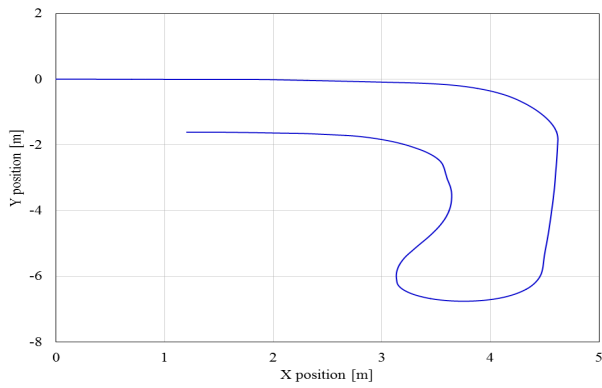
Where,  $\phi_{di}$  is the desired heading of the shortest path.

### IV. EXPERIMENTAL WORKS

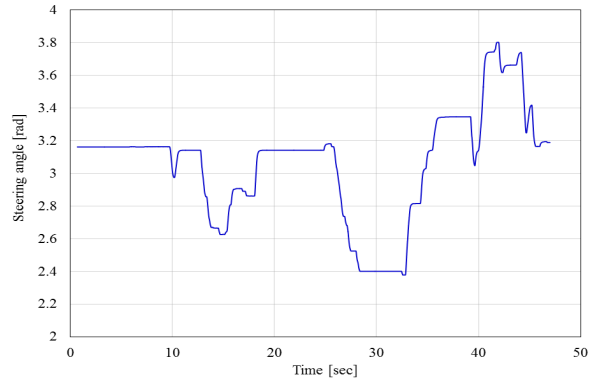
In this section, we tested the developed motion control of the modified system in two different cases and investigated the feasibility of the collision-free navigation algorithm which introduced in this research.

#### A. Navigation using joystick commands

This experiment conducted to check the validation of the motion control method that used to control the modified platform. In this experiment the robot was guided by using velocity commands from a joystick. Fig. 7 (a) shows the motion trajectory of the robot. Here, we guide the robot forward in a linear motion for about 3 meters then turned right and continued forward for about 4 meters then turned right twice before finally turned left and move forward for about 1.5 meters. Fig. 7(b) and (c) shows the linear velocity and angular velocity commands given by joystick, respectively. Fig. 7 (d) and (e) shows the robot's steering axis velocity and the steering angle during the motion experiment, respectively. As a result, the steering axis motor responded smoothly to the commands and the steering angle was consistent with the robot motion.

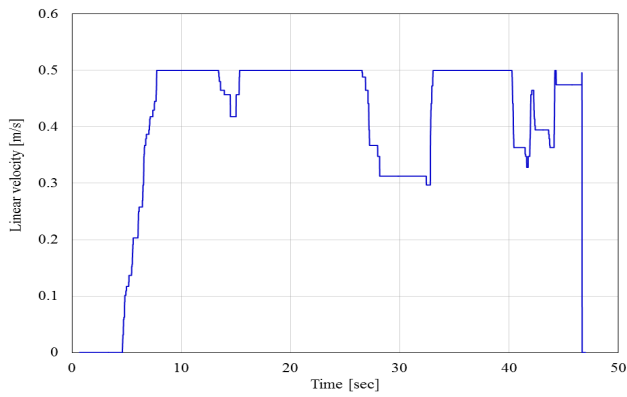


(a) Motion trajectory of the robot

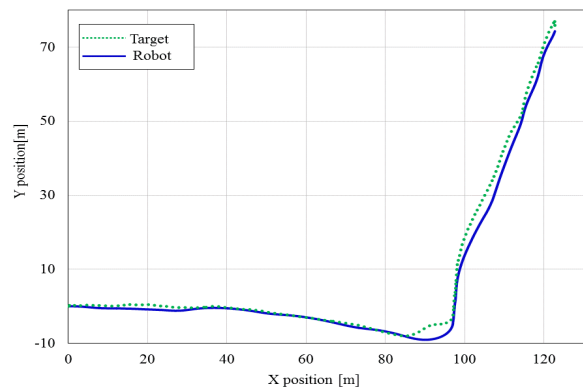


(e) Angle of the steering joint (measured)

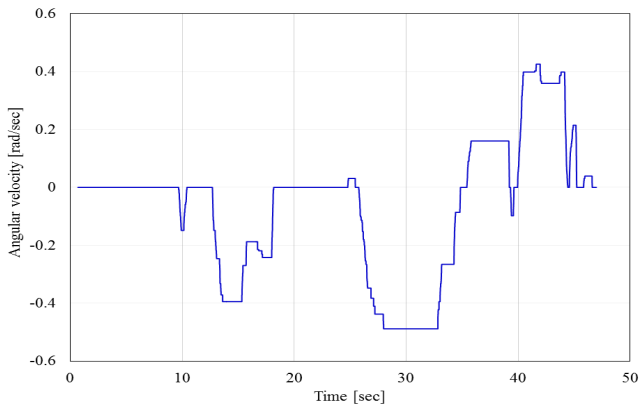
Fig. 7. Robot motion according to velocity command by joystick



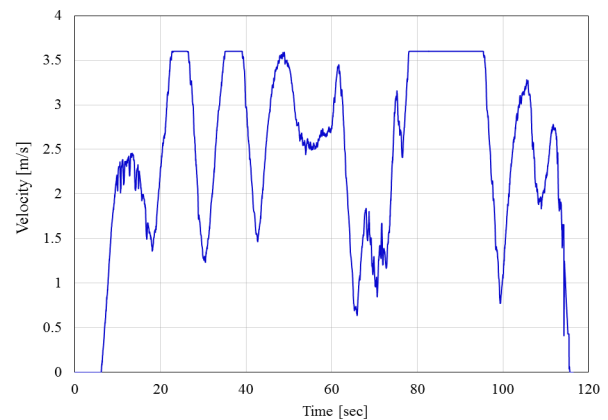
(b) Linear velocity command



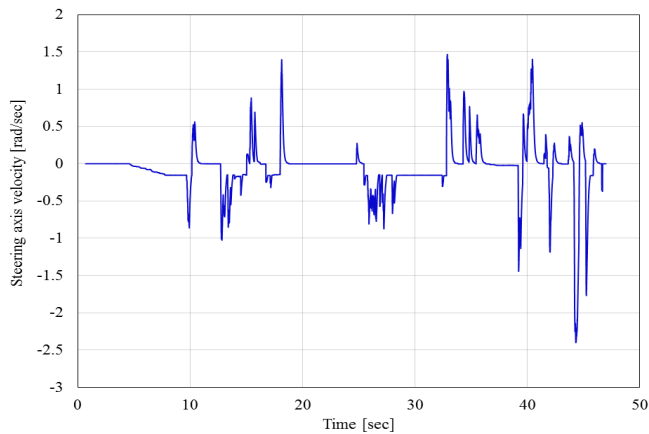
(a) Motion trajectories of the robot and the target person



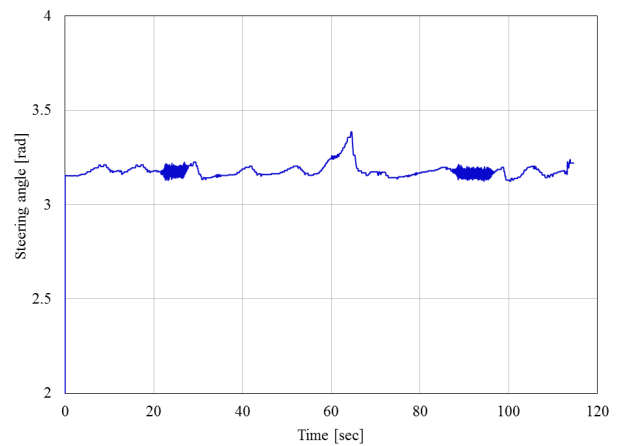
(c) Angular velocity command



(b) Linear velocity of the robot



(d) Angular velocity command of the steering joint



(c) Angle of the steering joint (measured)

Fig. 8. Running speed experimental results

### B. Running Speed Human Following

This experiment is conducted to check the validation of the vehicle's control method as a part of human following navigation system with no obstacle involved. Also this experiment conducted to check the ability of the modified system to navigate in high speed. Fig. 8 (a) shows the motion trajectories of the robot and target person. The motion control method was able to guide the robot to follow a target person without drifting for about 190 meters with speed up to 3.6 (m/s) as shown in Fig. 8 (b). Fig. 8 (c) shows the robot steering joint angle. There was some vibration in the robot steering axis (about -3 to +3 degrees) due to the irregularity of the outdoor terrain around second 25 and second 90, but it didn't affect the robot motion. As a result, the modified system was able to cope with the terrain irregularity and kept following a running person.

### C. Human Following with Static Obstacle



(a) t=0[s]



(b) t=4[s]



(c) t=7[s]

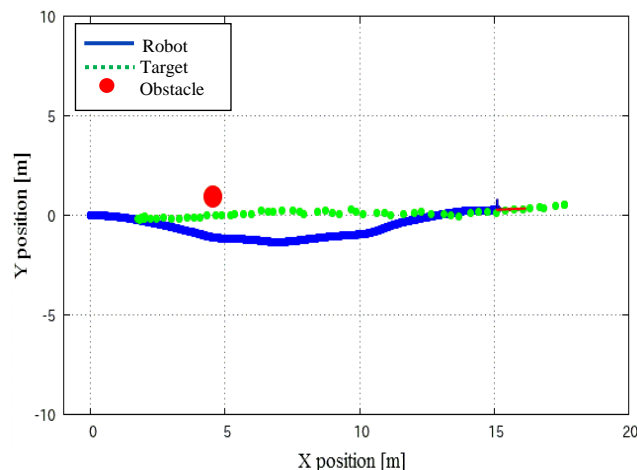


(d) t=9[s]

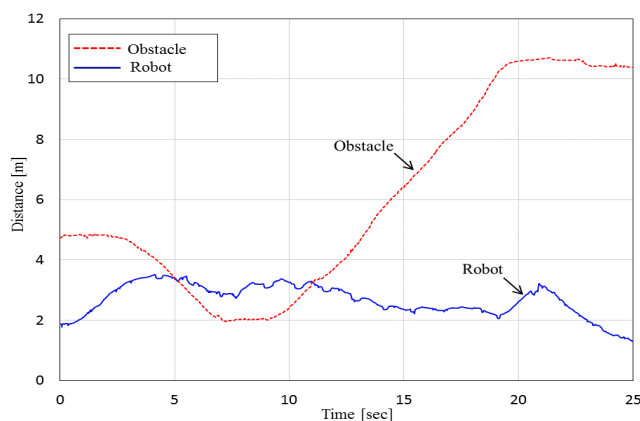


(e) t=13[s]

(a) Image samples captured during the experiment



(b) Motion trajectories of the robot, the target person, and the obstacle



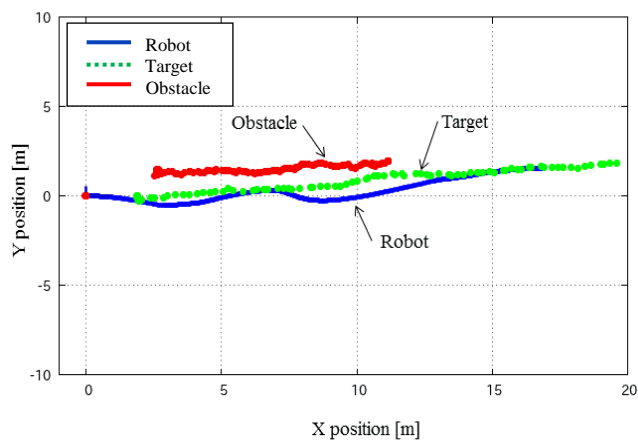
(c) Distance from the robot to the target and the obstacle

Fig. 9. Static obstacle avoiding experimental results

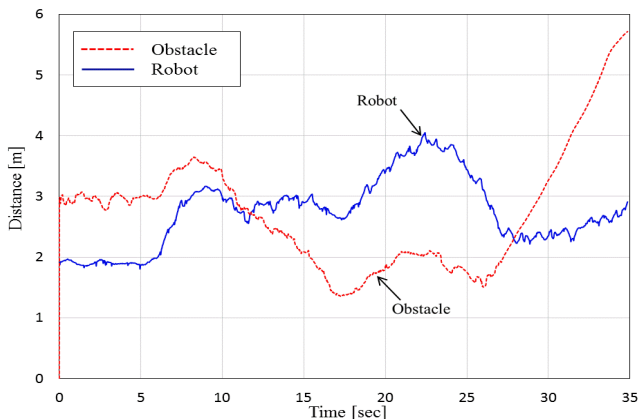
To show the effectiveness of the introduced algorithm to avoid collision with static obstacles while following a moving target person, this experiment was conducted in outdoor environment with passive front wheel. In this experiment we set a static obstacle about 5 meters away from the robot and the target person walked forward for about 15 meters. Fig. 9 (a) shows sample images of the experiment, captured by the omnidirectional camera installed on the robot and the operator's, the person in the green t-shirt represents the target person and the person in the orange t-shirt represent the static obstacle. Fig. 9 (b) shows the motion trajectories of the robot, target, and the obstacle. Fig. 9 (c) shows the distance between the robot and target person and the distance between the robot and obstacle during the experiment. Here we can see that the robot was trying to maintain a desired position which is 2 meters behind the target person and to keep a safety distance from the obstacle which is also 2 meters.

D. Human Following with Moving Obstacle

This experiment was conducted to show the effectiveness of the introduced algorithm to avoid collision with dynamic obstacles. This experiment conducted with passive front wheel. In this experiment, the target person walk forward for about 18 meters while an obstacle person walked beside him in a speed lower than the target person speed. The target person speed was about 0.8 (m/s) while the obstacle speed was about 0.4 (m/s). Fig. 10 (a) shows sample images of the experiment, captured by the omnidirectional camera installed on the robot and the operator's, the person in the green t-shirt represents the target person and the person in the orange t-shirt represents the static obstacle. Fig. 10 (b) shows the motion trajectories of the robot, target, and the obstacle. Fig. 10 (c) shows the distance between the robot and target person and the distance between the robot and obstacle during the experiment. Here we can see that whenever the obstacle gets close to the robot, the robot moved away and tried to keep the safety distance from the obstacle and also to maintain the desired position behind the target person.



(b) Motion trajectories of the robot, the target person, and the obstacle



(c) Distance from the robot to the target and to the obstacle

Fig. 10. Dynamic obstacle avoiding experimental results

V. CONCLUSIONS

In this paper, steering wheel design for a two wheeled mobile robot, kinematic modeling, and vehicle motion control method were discussed. Also, collision-free human following navigation considering static and dynamic obstacles was introduced. As a result, the new modified system showed a better performance and was able to follow a target moving with speed up to 3.6 (m/s). Also the feasibility of the introduced collision-free human following navigation algorithm was confirmed.

REFERENCES

- [1] G. Campion, G. Bastin, and B. D' Andéa-Novel, "Structural Properties and Classification of Kinematic and Dynamic Models of Wheeled Mobile Robots," IEEE Transactions on Robotics and Automation, vol.12.1, p47-62, 1996.
- [2] W. Kim, D. H. Kim, B.-J. Yi, B.-J. You, and S.-L. Yang, "Design of an Omni-directional Mobile Robot with 3 Caster Wheels," Transaction on Control Automation, and Systems Engineering, Vol. 3, No. 4, 2001.
- [3] J.A. Batlle, A. Barjau, "Holonmy in mobile robots," Robotics and Autonomous Systems, vol. 57. 4, p433-440, 2009.
- [4] D. Fox, W. Burgard, and S. Thrun, "The Dynamic Window Approach to Collision Avoidance," IEEE Robotics & Automation Magazine, vol.4.1, p23-33, 1997.
- [5] Wesley H. Huang, Brett R. Fajen, Jonathan R. Fink, and William H. Warren, "Visual Navigation and Obstacle Avoidance Using a Steering Potential Function," Robotics and Autonomous Systems vol.54.4, p288-299, 2006.
- [6] L. Hang, "Velocity Planning for a Mobile Robot to Track a Moving Target - a Potential Field Approach," Robotics and Autonomous Systems vol.57, p55-63, 2009.
- [7] T.-L. Lee and C.-J. Wu, "Fuzzy Motion Planning of Mobile Robots in Unknown Environments," Journal of Intelligent and Robotic Systems vol.37.2, p177-191, 2003.
- [8] X. Yang, R. V. Patel, and M. Moallem, "A Fuzzy-Braitenberg Navigation Strategy for Differential Drive Mobile Robots," Journal of Intelligent and Robotic Systems vol.47.2, p101-124, 2006.
- [9] F.-L. Lian, C.-L. Chen, and C.-C. Chou, "Tracking and Following Algorithms for Mobile Robots for Service Activities in Dynamic Environments," International Journal of Automation and Smart Technology, 2015.
- [10] E.-J. Jung, J. H. Lee, B. Yi, J. Park, S. Yuta, and S.-T. Noh, Development of a Laser Range Finder Based Human Tracking and Control Algorithm for a Marathoner Service Robot, IEEE/ASME Transactions on Mechatronics, Vol. 19, No. 6, 2014.
- [11] J. H. Lee, K. OKAMOTO, M. OUE, and S. OKAMOTO, Development of Outdoor Mobile Robot for Human Following Navigation, International Symposium on Artificial Life and Robotics, 2013.